IMPACT OF HOT COMPRESSED WATER PRETREATMENT ON THE STRUCTURAL CHANGES OF WOODY BIOMASS FOR BIOETHANOL PRODUCTION

Ling-Ping Xiao,[a] Zhao-Jun Sun, [b,]* Zheng-Jun Shi,[a] Feng Xu,[a,]* and Run-Cang Sun,[a,c]

As an initial step in an alternative use of woody biomass to produce bioethanol, this work was aimed at investigating the effect of hot compressed water (HCW) pretreatment within the temperature range 100 to 200 °C in a batch-type reactor on the structural changes of *Tamarix ramosissima*. The untreated and pretreated solid residues were characterized by X-ray diffraction (XRD), scanning electron microscopy (SEM), Fourier transform infrared spectroscopy (FT-IR), solid-state cross polarization/magic angle spinning (CP/MAS), ^{13}C NMR spectroscopy, and thermogravimetric analysis (TGA), as well as chemical methods. The results showed that HCW pretreatment solubilized mainly hemicelluloses and resulted in enriched cellulose and lignin content in the pretreated solids. It was found that the deposition of lignin droplets on the residual surfaces was produced during pretreatment under the hot water conditions above 140 °C. In addition, the removal of hemicelluloses and lignin re-localisation as a result of condensation reactions under harsh pretreatment condition may lead to an increase in cellulose crystallinity and thermal stability of biomass solid residues, thus consequently in favor of the available accessibility for enzymes actions. Finally results showed enzyme saccharification of HCW pretreated solids at the severest conditions assayed at 200 °C resulted in an enzymatic hydrolysis yield of 88%, which was improved by 3.4-fold in comparison with the untreated material.

Keywords: Tamarix ramosissima; Hot compressed water; Hemicellulose; Lignin; Cellulose

Contact information: a: Institute of Biomass Chemistry and Technology, Beijing Forestry University, Beijing 100083, China; b: Research and Development Centre for New Technology Application, Ningxia University, Ningxia 750021, China; c: State Key Laboratory of Pulp and Paper Engineering, South China University of Technology, Guangzhou 510640, China
**Corresponding author: xfx315@bjfu.edu.cn, nxszj168@sohu.edu*

INTRODUCTION

To solve global warming problems and ensure sustainable development of the economy and availability of oil feedstocks, it is necessary to increase the use of renewable biomass resources. Lignocellulosic materials, such as agro-industrial and forestry wastes, are natural complex composites primarily consisting of three biopolymers: cellulose (30-50%), hemicelluloses (20-35%), and lignin (10-25%) (Zhu et al. 2009). The accessibility of the cellulose, embedded in the plant cell wall with hemicelluloses and lignin, and the highly crystalline nature of the cellulose are two main factors that increase the cost associated with processing lignocellulosic biomass (Çetinkol et al. 2010). Pretreatment has been investigated as a means of modifying the cellulose

structure in such a way as to break down lignin, dissolve hemicelluloses, and disrupt the crystalline structure of cellulose. A major concern in lignocellulose conversion is overcoming biomass recalcitrance through pretreatment while still maintaining green and energy-efficient processing (Lee et al. 2009). The importance of developing a pretreatment process, for example, typically includes two factors: (1) conversion of the initial lignocellulosic material into an easily hydrolysable format, and (2) avoiding production of any degradation products or inhibitory compounds that will negatively impact the downstream processing of that treated biomass into biofuels (Singh et al. 2009). The initial characteristics of the woody biomass and the effect of subsequent pretreatment play significant roles in the development of substrate properties, which in turn govern the efficacy of enzymatic hydrolysis (Chandra et al. 2007). Various pretreatment technologies have been developed, including dilute acid, ammonia, steam explosion, ethanol organosolv, sulfite pretreatment (SPORL), and ammonia fiber explosion (AFEX) (Alizadeh et al. 2005; Gupta and Lee 2009; Pan et al. 2005; Sassner and Zacchi 2008; Wyman et al. 2005). However, they generally entail the use of either chemicals or high energy input, which make them not cost-efficient.

Recently, liquid water under elevated temperature and pressure, namely hot compressed water (HCW) or autohydrolysis or hydrothermal processing, has attracted considerable attention. The advantages are: corrosion problems are limited, no sludge is generated, capital and operational costs are low, and cellulose is not significantly degraded under normal operating conditions (Liu 2010). Liquid hot water has been shown to effectively pretreat lignocellulosic biomass by partially hydrolyzing the hemicelluloses and disrupting the lignin and cellulose structures, thus increasing the surface area (Mosier et al. 2005). During the HCW pretreatment, acetic acid is released from O-acetyl groups in the polysaccharides, which lowers the pH of the extract to the range 3-4 (Chen et al. 2010b). The hemicelluloses are then dissolved as oligomers after acid hydrolysis of the polymeric structures. Subsequently the hemicellulose oligomers in solution are partially further hydrolyzed to monomer sugars and sugar degradation products. Sugar degradation products include hydroxymethylfurfural (HMF) formed from hexose sugars and furfural formed from pentoses and uronic acids (Chen et al. 2010b). Lignin is partially depolymerized and solubilized as well during HCW pretreatment, but complete delignification is not possible using hot water alone, because of the recondensation of soluble components originated from lignin (Alvira et al. 2010).

In this study, *Tamarix ramosissima* was used as the lignocellulosic feedstock. The pruning of this shrub tree generates an abundant renewable lignocellulose residue, because stems of the plant are cut once every 3 or 4 years to make it flourish. Therefore, forest biomass can be harvested annually, which is a significant advantage over any agricultural biomass for the future biobased industry (Zhu et al. 2010). The efficient use of *Tamarix* can undoubtedly promote biodiversity and sustain a healthy forest ecosystem and meet regional bioenergy needs.

To date, however, comprehensive comparative analysis has been rarely conducted in order to investigate the HCW pretreatment process on the change of physical and chemical features of woody biomass. Furthermore, the mechanisms of how the HCW pretreatment acts on solid material, causing changes in solid features, disrupting the lignin-carbohydrate linkages, and thereby impacting subsequent enzymatic hydrolysis

have not been evaluated well. The primary objective of this work is to gain a better understanding of the impact of HCW pretreatment on solids and to judge the feasibility of such processing on downstream bioethanol production. Characterization of the untreated and pretreated solids was performed to determine glucan, xylan, and lignin contents of *Tamarix*. Physical chemical characteristics including cellulose crystallinity and plant cell wall morphology were also measured and compared using X-ray diffraction (XRD), scanning electron microscopy (SEM), Fourier transform infrared spectroscopy (FT-IR), solid-state cross polarization/magic angle spinning (CP/MAS) ^{13}C NMR spectroscopy, and thermogravimetric analysis (TGA).

EXPERIMENTAL

Materials

T. amosissima was harvested in Ningxia province, China, in 2009, from five-year-old plants. The leaves and bark were removed, and the trunks were chipped into small pieces. After drying at 60 °C for 16 h in an oven, the chips were then screened to obtain a 40 to 60 mesh fraction. Subsequently, the powder was dewaxed with toluene-ethanol (2:1 v/v) in a Soxhlet instrument for 6 h. The extractive free samples were further dried in a cabinet oven with air circulation at 60 °C for 16 h and stored in a sealed plastic bag and kept refrigerated (5 °C) until shortly before use. All weights and calculations were made on oven-dried basis. All chemicals were purchased from Sigma Chemical Co. (Beijing, China).

Methods

Hot compressed water pretreatment

HCW experiments were carried out in batch tube reactors fabricated from 316 stainless steel tubes having a length of 4.5 inches, an outside diameter of 1.0 inch, wall thickness of 0.065 inch, and a total volume of 50 mL. The reactor was filled with 3 g *Tamarix* power and 30 mL deionized water to achieve a 10% w/v of the dry matter mixture. Subsequently, the woody slurry was agitated for several minutes by a shaker until the pulverized powder was dispersed homogeneously. After the sample slurry was loaded, the 316 stainless steel caps were fitted onto each end of the tubes. Then an autoclave was used for heat-up of the tubes. HCW pretreatment of ground wood was obtained at temperatures in the range between 100 and 200 °C with 20 °C intervals. At the end of pretreatment, the reactor was cooled to room temperature. Subsequently, the entire reactor contents were emptied and separated into liquid and water-insoluble solid (WIS) fractions by vacuum filtration using a Buchner funnel lined with Whatman filter paper.

In order to analyze the original characteristics of untreated and pretreated materials, the reaction mixture was not washed with deionized water. Prior to being used to determine the subsequent chemical composition, the recovered solids were oven dried and employed for solid yield determination (expressed as g spent solid/100 g of untreated dewaxed material, on dry basis).

Characterization

Analytical methods

The typical compositions of dewaxed raw material and pretreated *Tamarix* were determined by use of a National Renewable Energy Laboratory's (NREL) standard analytical procedure (Sluiter et al. 2008) with minor modification. In brief, the cellulose and hemicelluloses content of the WIS fractions was determined based on monomer content after a two-step acid hydrolysis. A first step with 72% (w/w) H_2SO_4 at 30 °C for 60 min was used. In the second step, the reaction mixture was diluted to 4% (w/w) H_2SO_4 and autoclaved at 121 °C for 1 h. After cooling, the acid insoluble lignin (AIL) was collected by filtration, washed with deionized water until neutral pH eluate was obtained, and dried at 105 °C until constant weight. Absorbance reading of acid soluble lignin (ASL) was taken at 205 nm using a UV–Vis spectrophotometer with high purity quartz cuvettes with a 1 cm pathlength. The monomer sugars produced in the solutions were analyzed by high-performance anion exchange chromatography (HPAEC) (Dionex, ISC 3000, U.S.A) equipped with amperometric detector, AS50 autosampler, the CarbopacTM PA-20 column (4 × 250 mm, Dionex), and the guard PA-20 column (3 × 30 mm, Dionex). Neutral sugars and uronic acids were separated in a 5 mM NaOH isocratic (carbonate free and purged with nitrogen) for 20 min, followed by a 0-75 mM NaAc gradient in 5 mM NaOH for 15 min. Then the columns were washed with 200 mM NaOH to remove carbonate for 10 min, followed by a 5 min elution with 5 mM NaOH to re-equilibrate the column before the next injection. The total analysis time was 50 min and the flow rate was 0.4 mL/min. Calibration was performed with standard solutions of L-arabinose, D-glucose, D-xylose, D-rhamnose, D-mannose, D-galactose, glucuronic acid, and galacturonic acids. All samples were analyzed in duplicate. Monomeric sugars and degradation products in the hydrolysate were identified using modified NREL LAP "Determination of sugars, Bioproducts, and Degradation Productsd in Liquid Fraction Process Samples" (Sluiter et al. 2006). Briefly, carbohydrates in the water-soluble fraction after pretreatment were autoclaved with 4% sulfuric acid for 1 h at 121 °C to break down oligomeric sugars into monomeric. Glucose, xylose, arabinose, and galactose were quantified by HPAEC as described above. Inhibitors were analyzed on an Agilent 1200 HPLC equipped with an Aminex HPX-87H column (300 mm × 7.8 mm) and a refractive index detector (Bio-Rad Laboratories Inc., Hercules, CA). The mobile phase of the column was 0.005M sulfuric acid at a flow rate of 0.6 mL/min, with the column temperature at 50 °C.

Fourier transform infrared spectroscopy

Fourier transform infrared spectroscopy (FT-IR) was recorded from a FT-IR spectrophotometer (Tensor 27, Bruker, Germany). The samples (KBr pellets) for analysis were prepared by mixing 2 mg *Tamarix* powder with 200 mg KBr. Thirty-two scans were taken of each sample recorded from 4000 to 400 cm^{-1} at a resolution of 2 cm^{-1} in the in the transmission mode. The background spectrum of pure potassium bromide was subtracted from that of the sample spectrum.

Scanning electron microscopy

Scanning electron microscopy (SEM) of the untreated and pretreated residues was carried out with a Hitachi S-3400N II (Hitachi, Japan) instrument at 15 kV. Prior to taking pictures, the samples were sputter-coated with a thin layer of gold. Images were obtained at magnifications ranging from 200× to 3000×, which was dependent on the feature to be traced.

X-ray diffraction analysis

The crystallinities of untreated and pretreated *Tamarix* solids were measured using a XRD-6000 instrument (Shimadzu, Japan) with Cu Kα radiation source (λ=0.154 nm) at 40 kV and 30 mA. Samples were scanned at a speed of 1°/min, ranging from 2θ=5-40°, and a step size of 0.04° at room temperature. The crystallinity index (*CrI*) was calculated from XRD data and determined based on the formula by Segal et al. (1959) as follows,

$$CrI = 100 \times [(I_{002}-I_{am})/I_{002}] \quad (1)$$

in which I_{002} is the intensity for the crystalline portion of biomass (i.e., cellulose) at about 2θ=22.5, and I_{am} is the peak for the amorphous portion (i.e., cellulose, hemicellulose, and lignin) at about 2θ=18.7 in most literatures. It should be noted in this study that the second highest peak after 2θ=22.5 was at 2θ=16.4, and this was assumed to correspond to the amorphous region (Kumar et al. 2009; Li et al. 2010).

Solid state ^{13}C NMR spectroscopy

Solid state cross polarization/magic angle spinning (CP/MAS) ^{13}C NMR spectra of samples were obtained at 100.6 MHz using a Bruker AV-III 400 M spectrometer (Germany). Dry sample was packed in a 4 mm zirconia (ZrO_2) rotor, and the measurement was performed using a CP pulse program with 1 ms match time and a 2 s delay between transients. The spinning rate was 5 kHz. Calibration was done externally to the carbonyl carbon of glycine at 176 ppm.

Thermogravimetric analysis

Thermogravimetric analysis (TGA) was carried out on a Shimadzu TGA-60 instrument. Dynamic TG scans were conducted in a temperature range from 40 to 600 °C at a heating rate of 10 °C/min. The experiments were carried out under nitrogen atmosphere at a flow rate of 20 mL/min. Samples with approximately 8 to 11 mg of untreated and pretreated *Tamarix* were used.

Enzymatic hydrolysis

Enzymatic hydrolysis of the untreated *Tamarix* and pretreated substrates was performed according to a modified National Renewable Energy Laboratory (NREL) Laboratory Analytical Procedure (LAP) (Selig et al. 2008). Briefly, the hydrolysis was carried out at 50 °C on a rotary shaker at 200 rpm for 96 h. 200 mg of dry material was suspended to a 25 mL Erlenmeyer flask with 10 mL of 0.05 M sodium citrate buffer (pH 4.8). Approximately 4 mg of tetracycline chloride was used to control the growth of

microorganisms and prevent consumption of liberated sugars. Enzymes were added in the form of cellulose at 35 FPU/g substrates (Novozymes, NS50013, Bagsvard, Denmark) and β-glucosidase at 50 CBU/g substrate (Novozymes, NS50010, Bagsvard, Denmark). The concentration of the hydrolyzed monomeric sugars were determined by HPAEC under the same conditions as those described above. For clarity, error bars calculated based on the relative difference of duplicate experiments are not shown in time-dependent enzymatic hydrolysis yield plots in this paper.

RESULTS AND DISCUSSION

Compositional Analysis

Solid recovery of HCW pretreatment

In order to evaluate the efficiency of HCW as a pretreatment of *Tamarix*, the solid yield was calculated in relation to the raw material. The solid yields, which are shown in Table 1, ranged from 56% to 93%, and with values averaging 75% of the initial dry weight. As expected, due to the enhanced effect on the removal of water-soluble components, the overall solubilization of woody biomass increased under harsher conditions, which is consistent with the same trend in the literature (Kobayashi et al. 2009; Pérez et al. 2007).

Raw material composition

The composition of the biomass feedstock used for the pretreatment is presented in Table 1. The extractive-free *Tamarix* was found to have (dry matter, %) 30.3% of cellulose (as glucan) and 27.5% of hemicellulosic sugars with xylan as the main sugar (90%). Hemicelluloses of *Tamarix* are mainly composed of arabinoxylan with a high xylose content, as is usual in hardwood plants. Moreover, carbohydrates accounted for 65% of the whole plant, indicating that *Tamarix* is a potentially useful biomass resource for the production of biofuels and bio-based materials. Acid-insoluble lignin (AIL) and acid-soluble lignin (ASL) accounted for 15.1% and 9.2%, respectively. The lignin content of *Tamarix* is in the range of that reported for other forestry residues (Yu et al. 2008).

Composition of water-insoluble solid fractions

Analysis of chemical compositions of the *Tamarix* solids after HCW pretreatment showed significant differences compared to the untreated sample. The solid material recovered after HCW pretreatment mainly consisted of glucan and ASL, whereas the hemicellulosic sugars comprised a lower relative proportion of the carbohydrates in the treated wood as compared to the untreated material. Under the HCW pretreatment conditions, the hydronium ion initially causes xylan depolymerization and cleavage of the acetyl group. As a result, the acetyl group catalyzes the hydrolysis of the hemicelluloses and then the autohydrolysis reaction follows (Liu and Wyman 2004). The main effect of the HCW pretreatment on the composition of the biomass is the partial but substantial removal of hemicelluloses. Increasing the reaction temperature produced higher solubilization of xylan to a minimum amount of 2.7 g/100 g of raw *Tamarix* at 200 °C for 3 h, corresponding to 89% of the xylan in the raw material being solubilized. It was found

that other hemicellulosic sugars, such as arabinan and galactan, were almost completely removed at the higher temperatures. Consequently, with the content of hemicelluloses solubilized into prehydrolyzate, a cellulose enriched-WIS fraction was obtained. The total cellulose content increased ranging from 37% to 43%, when compared with the initial percentage of 30%. Overall, the solubilized xylan increased significantly with the raising temperature.

The recovered WIS fractions were found to have a significantly higher level of lignin content as compared to the untreated *Tamarix*. Concerning the lignin content, the maximum value of pretreated material reached 40% under the harsh condition of 200 °C for 3 h. The acid-insoluble lignin decreased firstly with temperature and then increased to 40.1%, which was even higher than those in the untreated woody biomass. This is comparable with the results recently reported by Lü and Saka (2010), who also found that the same changing tendency of acid-insoluble lignin as Japanese beech was treated by batch hot-compressed water. A similar result was reported by Cara et al. (2007), who obtained lignin recovery values that exceeded initial concentration (19 to 39%) when pretreating olive tree pruning residues with liquid hot water in the range of 170 to 230 °C for 10 or 60 min. The relatively high content of lignin may be related char or other possible repolymerization or condensation products formed under the severe pretreatment conditions (Cara et al. 2007; Lü and Saka 2010).

Water-soluble fraction composition

During HCW pretreatment, water acts as a weak acid and promotes rapid acid-catalyzed hydrolysis of polysaccharides to monosaccharides, which subsequently degrade to furfural, hydroxymethylfurfural (HMF), and other inhibitors.

As shown in Fig. 1, total glucose production of water-soluble fraction increased with temperature when the temperature was lower than 140 °C, with the maximum production (2.8 g/L) was attained. When the temperature was increased over 160 °C, the production of glucose began to decrease with temperature. Likewise, total xylose production increased with increasing temperature, peaked at 160 °C, and decreased to almost zero at higher temperature due to degradation. The maximum production amounted to 46 g/L. In addition, the production profiles of total arabinose and galactose were similar, sugar production peaking at 160 °C, but their amounts were much lower than the total glucose and xylose produced. Moreover, the yield of inhibiting products resulted in prehydrolyzating concentrations of 2.7 g/L and 1.7 g/L for acetic acid and furfural under the most severe conditions (data not shown).

The quantity of levulinic acid found was negligible, and the HMF yield was always < 0.09 g/L (data not shown). Based on the above results, it is clearly shown that the post-hydrolysis of the liquid products have a high glucose and xylose production, which further could be fermented to produce biofuel (Yu and Wu 2010). Moreover, the production of acetic acid and furfural indicated that HCW pretreatment significantly broke down the woody biomass structure, especially at higher temperature and longer pretreatment time (Yu et al. 2010).

Table 1. Solid Yield, Composition (dry matter, %) and Crystallinity Index (*CrI*) of Untreated and Pretreated ***Tamarix***

	Untreated	Temperature (°C)					
		100	120	140	160	180	200
Solid yield	100.0	93.2	90.1	85.0	67.2	60.6	56.6
Glucan	30.3 ± 1.7	36.5 ± 3.5	33.6 ± 0.9	31.8 ± 4.2	38.5 ± 0.4	40.2 ± 1.2	42.9 ± 3.1
Xylan	24.9 ± 0.5	30.9 ± 3.9	29.0 ± 0.1	29.2 ± 0.2	22.1 ± 0.2	11.8 ± 0.3	2.7 ± 0.6
Arabinan	1.0 ± 0.0	1.1 ± 0.1	0.9 ± 0.1	0.4 ± 0.0	0.2 ± 0.0	0.1 ± 0.0	Trace
Galactan	0.3 ± 0.0	0.4 ± 0.1	0.3 ± 0.0	0.3 ± 0.0	0.2 ± 0.0	0.1 ± 0.0	ND*
Rhamnan	0.3 ± 0.0	0.4 ± 0.1	0.3 ± 0.0	0.3 ± 0.0	0.1 ± 0.0	0.1 ± 0.0	ND
GluA**	0.7 ± 0.0	0.9 ± 0.1	0.8 ± 0.1	0.8 ± 0.1	0.2 ± 0.0	0.1 ± 0.1	0.1 ± 0.0
GalA***	0.2 ± 0.1	0.2 ± 0.0	0.2 ± 0.0	0.2 ± 0.0	0.2 ± 0.0	0.1 ± 0.0	0.1 ± 0.0
Total lignin	23.5 ± 0.9	25.4 ± 1.3	24.6 ± 1.1	25.2 ± 0.9	31.7 ± 1.4	33.7 ± 0.8	41.5±0.3
Acid-insoluble	15.1 ± 1.4	11.0 ± 0.5	11.5 ± 0.4	14.1 ± 0.7	24.0 ± 2.1	29.3 ± 2.7	40.1 ± 0.6
Acid-soluble	9.2 ± 0.5	14.7 ± 0.9	13.1 ± 0.7	11.0 ± 1.6	7.7 ± 0.7	4.5 ± 0.9	1.4 ± 0.3
CrI	41.0	41.7	42.0	45.4	50.6	51.4	55.5
* ND, Not detectable; ** GluA, Glucuronic acid; *** GalA, Galacturonic acid.							

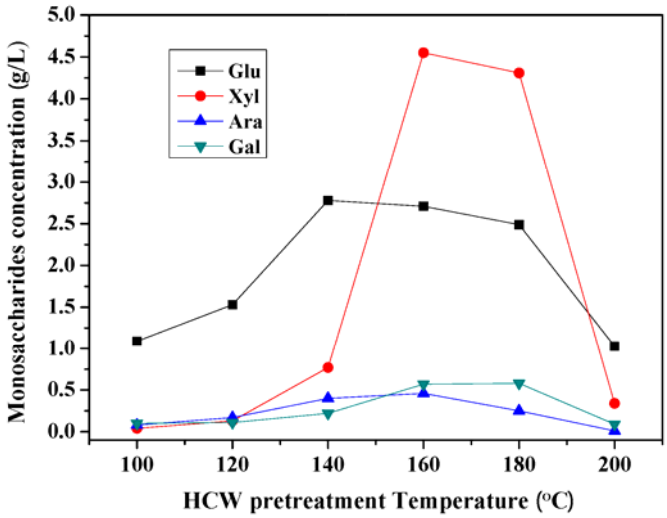

Fig. 1. Contents of glucose, xolose, arabinose and galactose of water-soluble fraction after HCW pretreatment at various temperatures for 3 h

Biomass Crystallinity

The degree of crystallinity and changes in the crystal structure of cellulose have been well established as two of the main determining factors in the efficacy of enzymatic hydrolysis of biomass (Çetinkol et al. 2010). Several factors related to a higher *CrI* of the substrate may contribute to the reduction of digestibility at the lower enzymatic loading: the decrease in the reactivity of the substrate during hydrolysis; different kinds of enzyme inactivation; and non-specific adsorption of enzymes onto lignin (Vlasenko et al. 1997). Figure 2 shows the XRD spectra of untreated *Tamarix* and pretreated solid residues obtained at different pretreatment temperatures. Overall, the peak intensity of cellulose crystal of solid residues between the temperatures of 100 °C and 200 °C did not show much difference when compared with that of untreated woody powder. The XRD measurements for solid residues thus demonstrated that the cellulosic crystalline structures could remain with little change during the HCW pretreatment. Nevertheless, it was found that the *CrI* of pretreated *Tamarix* significantly increased, caused by severe conditions, when compared to that of untreated *Tamarix* (Table 1). It has been suggested that hemicelluloses are eliminated from the surface by hydrolysis and cellulose undergoes changes in crystallinity upon chemical and physical treatment, particularly heating (Inoue et al. 2008; Lee et al. 2010). Higher values implied removal of more hemicelluloses and leaving the crystalline cellulose fraction intact in the HCW pretreated solid residues (Inoue et al. 2008). One additional possibility is that the cellulose in biomass may consist of a wide range of segments, containing both amorphous and crystalline portions. Recently, Yu and Wu (2011) have demonstrated that in the course of conversion processes the amorphous portion and segments with short chains that are more reactive may be reacted first, leaving a residual that has large sizes and is more inert. Solubilization of hemicelluloses and lignin together with less ordered cellulose is probably the main reason for the increase in cellulose crystallinity.

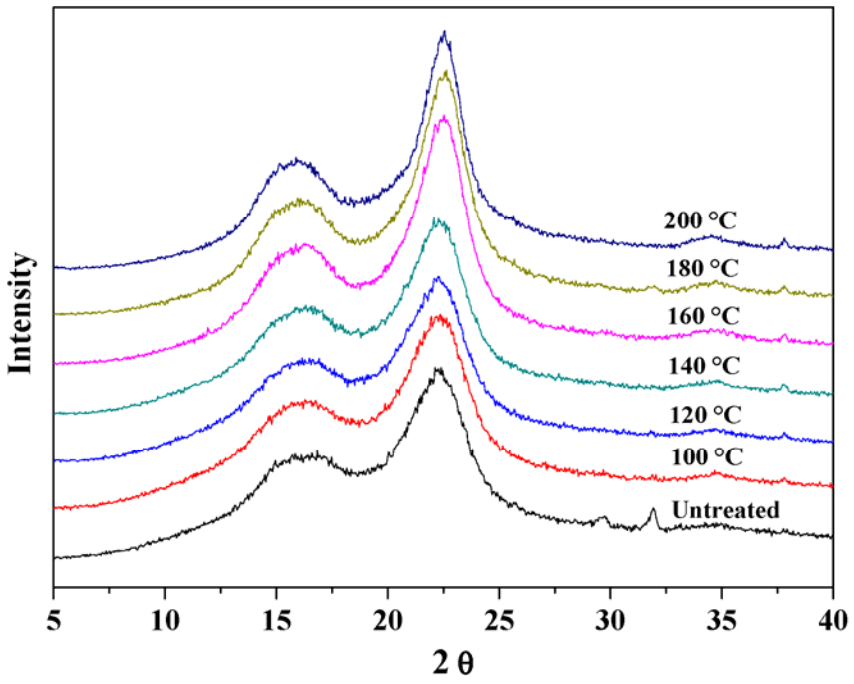

Fig. 2. XRD patterns of untreated and pretreated solid residues at various temperatures for 3 h

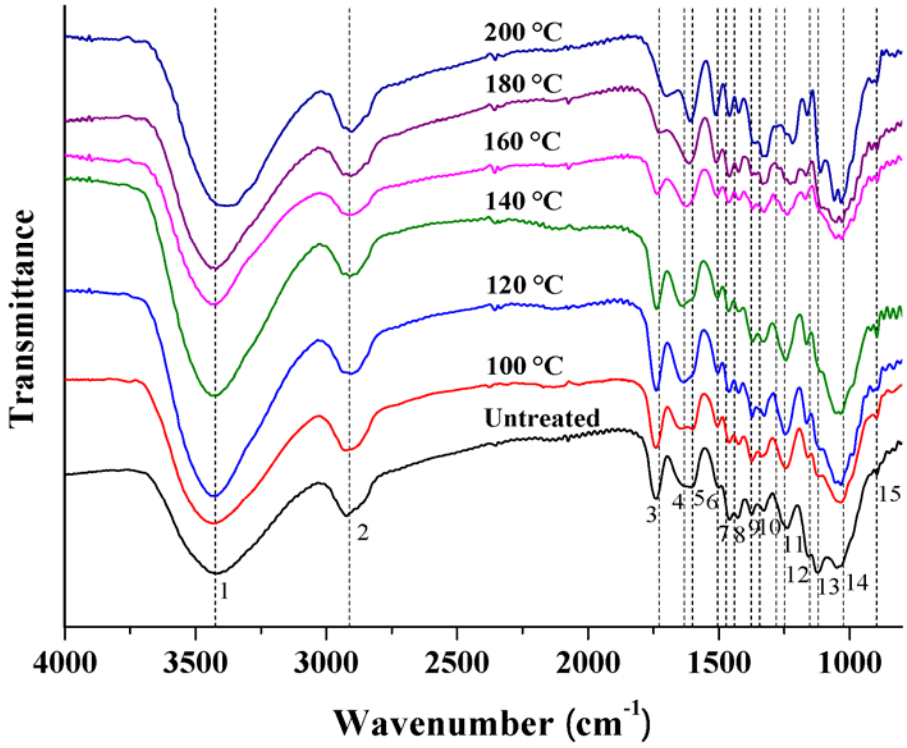

Fig. 3. FT-IR spectra of untreated and pretreated solid residues at different temperatures

Table 2. Assignments of Bands in Fourier Transform Infrared Spectra of Untreated and Pretreated *Tamarix*

Band number	Wavenumber (cm^{-1})	Assignments
1	3418	–OH stretching
2	2924	–CH stretching of $–CH_2$ and $–CH_3$
3	1740	C=O stretching of unconjugated ketone, carbonyls, and ester groups; C=O in xylan acetates (hemicelluloses)
4	1643	Absorbed O–H and conjugated C–O
5	1605	Aromatic skeletal vibrations plus C=O stretch
6	1501	Aromatic C=C stretching from aromatic ring of lignin
7	1460	Aromatic C–H deformation; asymmetric in $–CH_3$ and $–CH_2–$
8	1427	Aromatic skeletal vibrations combined with C–H in plane deformation
9	1374	Aliphatic C–H deformation vibrations in cellulose and hemicellulose
10	1328	Phenolic OH; Syringyl ring plus guaiacyl ring condensed
11	1239	Syringyl ring breathing and C–O stretching out of lignin and xylan
12	1157	C–O–C vibrations at β-glucosidic linkages in cellulose and hemicellulose
13	1124	C–O, C–C stretching or C–OH bending in cellulose and hemicellulose
14	1049	C–O stretching in cellulose and hemicellulose
15	896	C–O–C stretching at β-glucosidic linkages in cellulose and hemicellulose

FT-IR Analysis

The FT-IR spectra of untreated and pretreated solids under HCW pretreatment are illustrated in Fig. 3, and peak assignments based on literature values are summarized in Table 2 (Çetinkol et al. 2010; Kobayashi et al. 2009; Kumar et al. 2009; Wang et al. 2010). As can be seen, the intensity of the carbonyl band at 1740 cm^{-1}, which has been ascribed to C=O of acetyl groups and other carbonyl groups of carboxylic acids in hemicelluloses (Çetinkol et al. 2010; Delmotte et al. 2008; Wang et al. 2010), becomes weaker with increasing reaction temperature. This is in reasonable agreement with removal of a large portion of the hemicelluloses, as shown in Table 1 and in Kristensen et al. (2008) and Kobayashi et al. (2009). The peak band around 1640 cm^{-1} decreases with increasing reaction temperature, and then the peak cannot be detected when the temperature was above 160 °C. This result suggests that the wood structure, where the moisture always forms hydrogen bonds, is totally broken down during the higher temperature of HCW pretreatment (Kobayashi et al. 2009). As compared to the untreated *Tamarix*, lignin band at 1501 cm^{-1} (aromatic ring of lignin) is significantly enhanced in the HCW pretreated samples. According to Kristensen et al. (2008), this phenomenon can be reasonably explained in two ways. One is that hemicelluloses are removed; the other is that lignin is released and re-deposited on the surface, which can be seen from the SEM micrographs as discussed below. It is noticeable in Fig. 3, that the peaks around 1239, 1427, 1501 and 1740 cm^{-1} were still visible with a reinforced intensity even at the high pretreated temperature of 200 °C for 3 h. These results are consistent with the compositional data in Table 1, where the pretreated samples have higher lignin contents.

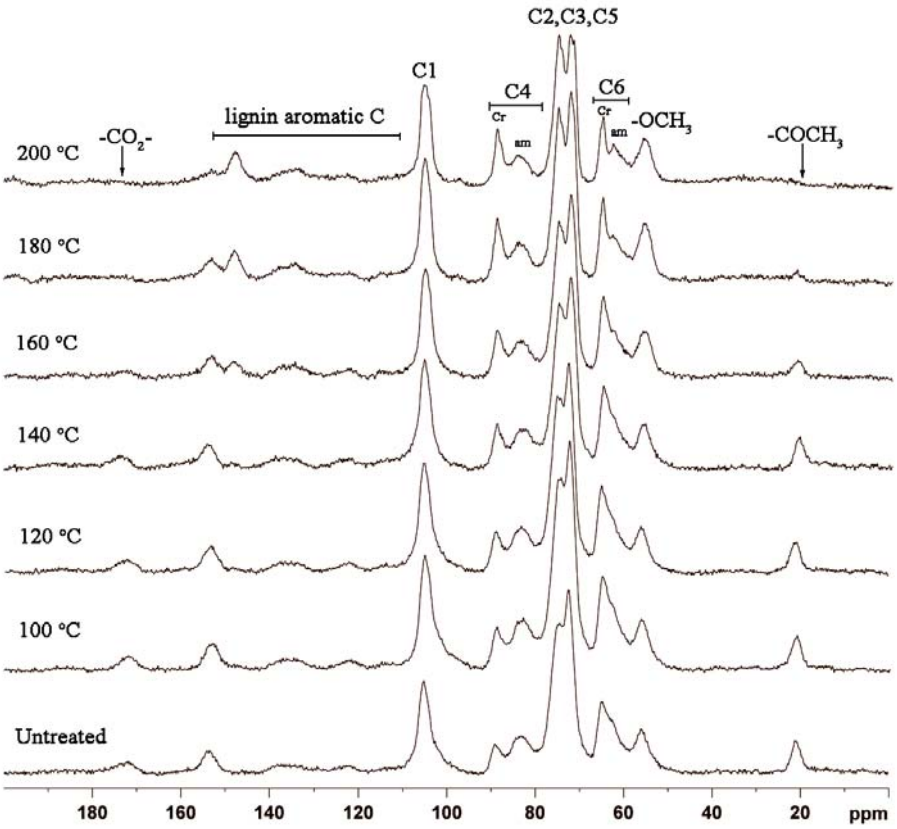

Fig. 4. ^{13}C CP/MAS NMR spectra of untreated and pretreated solid residues at various temperatures for 3 h. Cr refers to crystalline, am to amorphous.

Table 3. Signal Assignments for ^{13}C CP/MAS NMR Spectra of Untreated and Pretreated *Tamarix*

Chemical shift (ppm)	Types of carbons
172.3	–CO_2– in acetyl groups of hemicelluloses
153.3	S3 (e)*, S5 (e), G4 (e) in lignin
148.1	S3 (ne)**, S5 (ne), G3 in lignin
136.5	S1 (e), S4 (e), G1 (e) in lignin
133.8	S1 (ne), S4 (ne), G1 (ne) in lignin
122.2	G6 in lignin
115.6	G5 in lignin
113.8	G2 in lignin
105.4	C–1 of cellulose
101.7	Shoulder of C–1 of hemicelluloses
89.1	C–4 of crystalline cellulose
84.6	C–4 of amorphous cellulose
75-72	C–2, C–3, and C–5 of cellulose
65.2	C–6 of crystalline cellulose
62.9	C–6 of amorphous cellulose
56.2	–OCH_3 in lignin
21.4	–CH_3 in acetyl groups of hemicelluloses
* e, etherified; ** ne, nonetherified.	

Solid State NMR Analysis

The ^{13}C CP/MAS NMR spectra of the untreated and pretreated wood solids are shown in Fig. 4. The chemical shift assignments of the spectra of wood were made on the basis of literature data (Delmotte et al. 2008; Popescu et al. 2011; Wikberg and Maunu 2004; Nuopponen et al. 2006), and the outcome is summarized in Table 3. Overall, cellulose, hemicelluloses, and lignin gave characteristic signals in the solid state NMR spectra shown in Fig. 4.

Cellulose

The region between 60 and 110 ppm was dominated by strong signals, which were assigned mostly to various cellulosic carbons. Obvious signals for amorphous and crystalline carbons could be detected. The sharp signals at 105.4 ppm, 89.1 ppm, and 65.2 ppm correspond to the ordered cellulose C–1, C–4, and C–6 carbons, respectively, while the signals at 84.6 ppm and 62.9 ppm are due to the disordered cellulose C–4 and C–6 carbons (Wikberg and Maunu 2004). The signals at 72-75 ppm are assigned to cellulose C–2, C–3, and C–5. Difference in relative signal intensities could be seen as the pretreatment temperature increased. In particular, the intensities of the signal at 105.4 ppm corresponding to C–1 of cellulose were altered by the hydrothermal degradation.

Hemicelluloses

Furthermore, the relative intensity of the signals of 21.4 and 172.3 ppm, corresponding to methyl and carboxylic groups of the acetyl functions of hemicelluloses, decreased gradually as the temperature increased and then almost disappeared at the severest conditions of pretreatment temperature of 200 °C. This phenomenon evidently confirmed the removal of hemicelluloses during HCW pretreatment. Moreover, the analogous results were reflected in the compositional analysis data in Table 1 and FT-IR spectra in Fig. 3.

Lignin

The broader region between 110 and 155 ppm, which is specific for aromatic carbons of lignin, revealed large distinctions. As shown in Fig. 4, signals at 153.3 ppm are assigned to the C–3 and C–5 carbons of S and C–4 carbon of G units, which were etherified at C–4 (Nuopponen et al. 2006). A signal at 148.1 ppm is assigned to the C–3 and C–5 carbons in nonetherified S units and the C-3 carbons of G units (Nuopponen et al. 2006). Herein the signal at 153.3 ppm is mainly from the S units, which had β-O-4 linkages, and the signal at 148.1 ppm is mainly assigned to G units. In addition, the signal at 136.5 ppm is assigned to C–1 and C–4 carbons of S and the C–1 carbon of G units that are etherified, whereas the corresponding nonetherified structures give a shoulder at 133.8 ppm (Nuopponen et al. 2006). Evidently, a reduction in the relative intensity of the signal at 153.3 ppm and an increase in the relative intensity of the signal at 148.1 ppm were observed in all the solids before and after HCW pretreatment. One plausible explanation is that the Cα-Cβ bond and β-O-4 linkages in lignin were cleaved during hydrothermal modification and the heat steam treatment process, which partially depolymerises wood lignin by hydrolysing the aryl-ether linkages involving C–4 of syringyl and guaiacyl units (Popescu et al. 2011; Wikberg and Maunu 2004). Moreover,

the relative intensity of the signal at 56.2 ppm, corresponding to the methoxyl groups (–OCH_3) of aromatic moieties in lignin, decreased with the pretreatment temperature increased and then almost disappeared at the temperature of 200 °C. Demethoxylation of lignin makes more lignin sites available for reaction, and therefore a more condensed lignin structure is achieved (Wikberg and Maunu 2004).

Accordingly, comparing these results obtained from the ^{13}C CP/MAS NMR spectra, we can draw a conclusion that the main changes occurring in the chemical structure of wood solids during HCW pretreatment were due to the degradation of hemicelluloses simultaneously with striking changes in lignin structure. Wood lignin was broken down by intensive cleavage of β-O-4 linkages and Cα-Cβ bonds, and the demethoxylation of lignin led to a more condensed lignin structure.

Morphological Characteristics

Scanning electronic micrographs of the different *Tamarix* samples were obtained to verify the material structural changes caused by the HCW pretreatment (Fig. 5). The SEM micrographs Fig. 5A-G show the surfaces of *Tamarix* fibers before and after HCW pretreatment, where significant differences are observed. The untreated sample exhibited essentially regular and compact surface structure, and a highly fibrillar and intact morphology (Fig. 5A). Higher severity resulted in defibration of many ground fibers (Fig. 5B), together with more serious structural breakdown, and some cracks were also apparent on the particle surface (Fig. 5C). At a higher pretreatment temperature, considerable damage to the fibers could be observed clearly (Fig. 5D and E). The surface is uneven and covered with small debris and droplets, which are ascribed to the molten lignin at the high temperature and compressed pressure and subsequent condensation. The surface of the sample pretreated at the harsher condition (Fig. 5F and G) has numerous uneven folds and spherical and globular shapes, which were attributed to the deposited lignin as reported in the literature (Kristensen et al. 2008). This interpretation is consistent with the compositional analysis of higher AIL concentrations, as shown in Table 1. HCW pretreatment disrupts the lignocellulosic structure by mainly dissolving hemicelluloses. As a result, the major microfibrous cellulose structures were still preserved (Fig. 5G), and some lignin or lignin carbohydrate complexes may be condensed on the surface of the cellulose fibers (Zhu et al. 2009). Herein microfibrils were not completely fibrillated but remained bonded to polymer matrix, and their surface structures were changed from fibrous to twisted shapes.

Interestingly, perfectly granular and globular lignin particles can be clearly observed on the surface of residual biomass (Fig. 5D to G). The droplet density produced from the lignocellulosic biomass during HCW pretreatment generally increased with elevated pretreated temperature between 140 °C and 200 °C. Under the hot water conditions, the observed droplets coalesced into lignin globules of various sizes ranging from 0.2 to 70 μm in diameter. Selig et al. (2007) hypothesized that upon melting, lignins in biomass become fluid and coalesce, and have the potential to move throughout the cell wall matrix; the cited authors observed spherical formations on the surface of pretreated corn stover during the high-temperature pretreatment process.

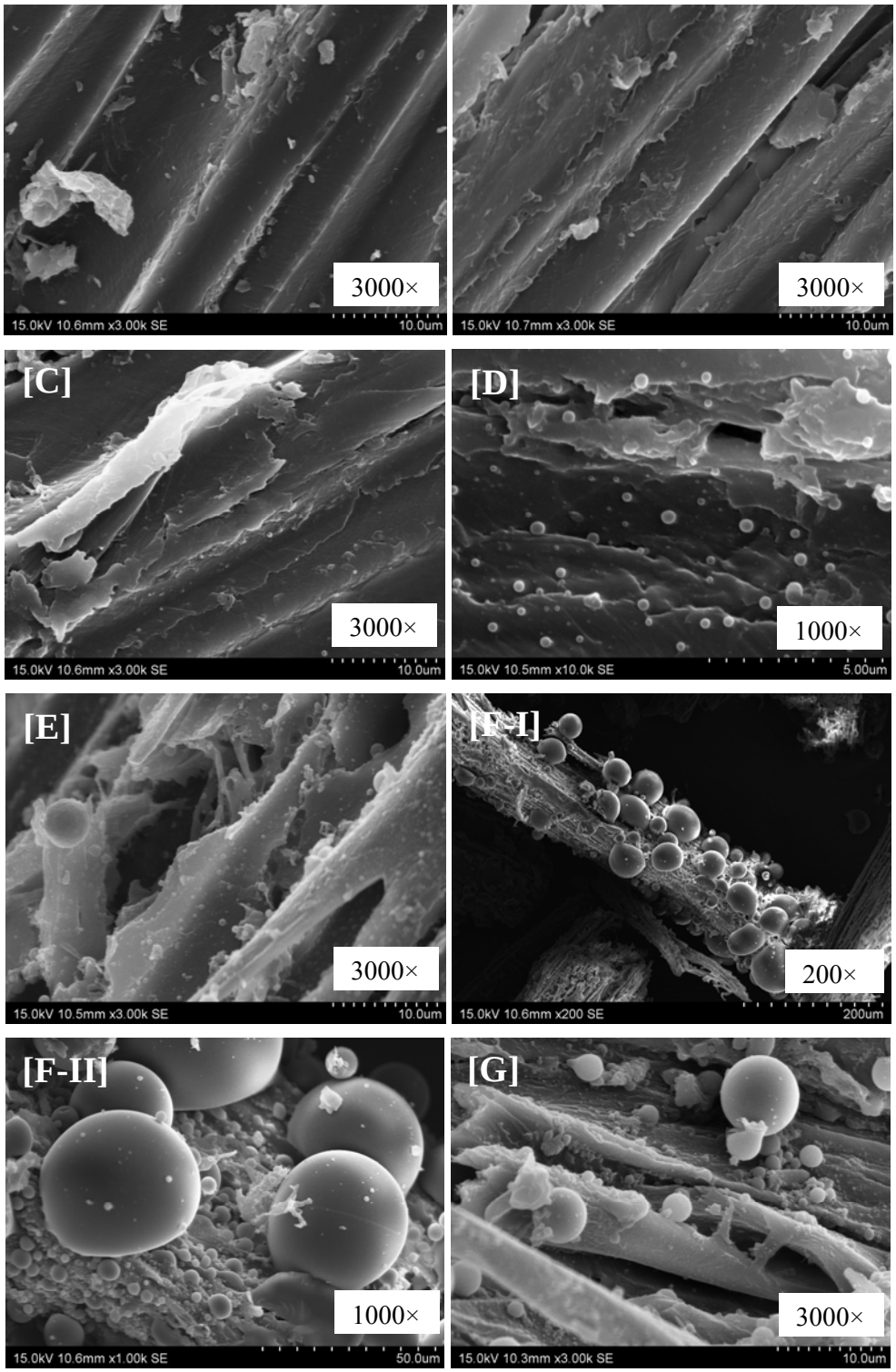

Fig. 5. SEM images at various magnifications for untreated and pretreated *Tamarix*. [A] untreated raw material at 3000× and pretreated *Tamarix* at different temperatures for 3 h: [B] 100 °C at 3000× , [C] 120 °C at 3000× , [D] 140 °C at 1000× , [E] 160 °C at 3000× , [F] 180 °C at 200× (I), 1000× (II), and [G] 200 °C at 3000×.

Xu et al. (2007) also found that a large amount of lignin particles were precipitated on the fibers after ethanol-based organosolv pulping, and the colloidal structural of lignin could form a glassy coating that adhered to the wood structure. Therefore, the lignin droplets observed when the reaction temperature was above 140 °C, in this study on the pretreated *Tamarix*, is in accordance with the results found in the literature (Donohoe et al. 2008; Selig et al. 2007; Xu et al. 2007; Zeng et al. 2007). Moreover, the re-localisation of the lignin as reflected in the SEM images is consistent with the results of high lignin content in Table 1 and reinforced lignin related intensity in FT-IR and ^{13}C CP/MAS NMR spectra in Figs. 3 and 4, respectively.

Thus, based on the differences from SEM micrographs, it is evident that HCW pretreatment resulted in breakage of the matrix fibrous polymers network and partial defibrillation, as well as partial removal of hemicelluloses and lignin re-localisation. Moreover, high-temperature pretreatments have a significant impact on the state of lignin. Accordingly, it is demonstrated that deposition of lignin droplets was produced during pretreatment under hot water conditions, and above 140 °C they can redeposit as spherical droplets on the residual surfaces.

Thermal Analysis

In order to understand the changes in the thermal properties of materials before and after HCW pretreatment, the TGA, DTA, and DTG of untreated and treated pre-treated *Tamarix* were measured. Thermogravimetric analysis (TGA) and first derivative thermogravimetric (DTG) curves are presented in Fig. 6. These three curves together describe the behavior of the samples subjected to pyrolysis under nitrogen atmosphere.

Overall, in regard to the TGA distributions of the untreated and pretreated solids (Fig. 6Aa to Ad), their profiles were found to be similar with each other. Specifically, the curves dropped dramatically when the TG's heating temperature increased from 250 to 400 °C. As clearly shown from the TGA and DTA profiles, with the increase of pretreatment temperature, the thermal stability increased continuously, evidenced by the gradually higher rising decomposition temperature to an extent of about 10-70 °C, and the ceaselessly reduced carbon residue at an elevated temperature. For example, the carbon residue's degradation temperature at *ca.* 50% weight loss was 323 °C for the untreated material, compared with 332 °C, 345 °C, and 355 °C for the pretreated samples, respectively. Moreover, HCW pretreatment of *Tamarix* shifted the main thermal decomposition peak to a higher temperature region (347 to 471 °C for the untreated material vs. 365 to 575 °C for the pretreated solids) at a higher severity.

From the DTG (first derivative) profile for the rate of weight loss, the behavior of untreated *Tamarix* shows four distinct peaks, indicating that the degradation can be explained by dividing the curves into four stages. As shown in Fig. 6C, the initial mass loss at about 62 °C is due to the moisture present in the sample. In the second stage from 239 to 305 °C with a maximum weight loss rate attained at 300 °C is ascribed to hemicellulose degradation. The third stage occurred from 305 to 361 °C, with a maximum decomposition rate at 325 °C, which is attributed to the decomposition of cellulose. Compared with these three components, lignin was the most difficult one to decompose. Its decomposition occurred slowly in the fourth stage with a maximum decomposition rate at 465 °C.

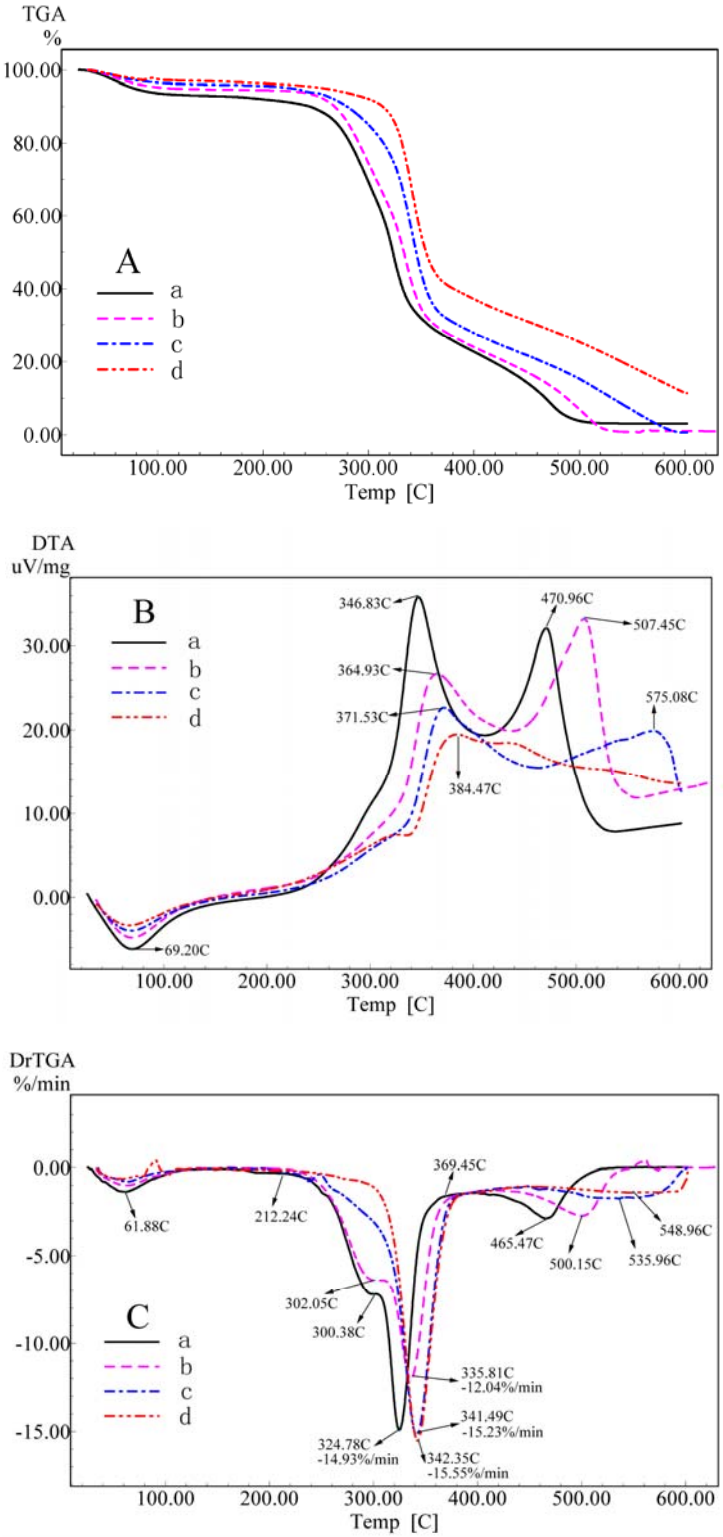

Fig. 6. (A) TGA, (B) DTA, and (C) DTG distributions of the untreated and pretreated *Tamarix* before and after HCW pretreatment: (a) untreated material; (b) pretreated at 120 °C for 3 h; (c) pretreated at 160 °C for 3 h; (d) pretreated at 200 °C for 3 h; N_2 atmosphere, 20 mL/min, 10 °C/min

These observations are consistent with results reported in the literature (Chen et al. 2010a; Spinacé et al. 2009; Yang et al. 2006). Consequently, the observed behavior is in accordance with the chemical component analysis listed in Table 1, qualitatively confirming the contents of carbohydrates and lignin in the raw material. The thermal degradation behavior of samples pretreated at 120 °C, Fig. 6Cb, has the same trend as that of raw *Tamarix*. It is worth noting that the peaks of DTG distribution moved leftward to a higher temperature and the reaction intensity was decreased. In particular, once the HCW pretreatment temperature increased to 160 °C and 200 °C, the overlapped double-peak distribution evolved into a single-peak distribution, and the peak moved leftward to around 340 °C, together with a small shoulder at a higher temperature around 550 °C. This result can be explained in that after the HCW pretreatment, the peaks related to thermal decomposition of cellulose (third peak) and lignin (fourth peak) shifted to a higher temperature. Due to the HCW pretreatment, the hemicelluloses and partially cellulose as well as some lignin were removed and degraded, as previously mentioned, hence substantially altering the lignocellulosic structure and then facilitating the thermal decomposition of HCW pretreated solids.

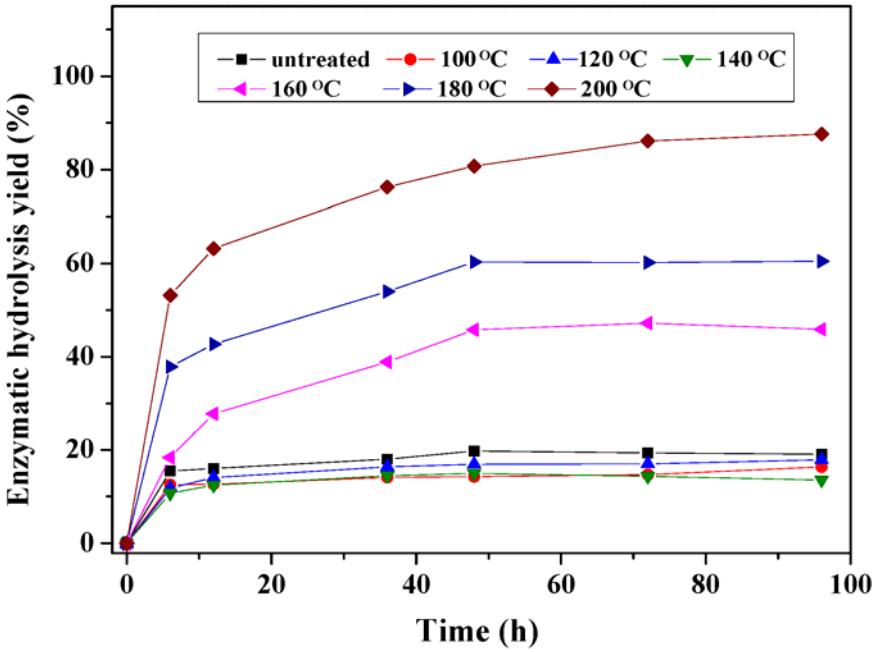

Fig. 7. Enzymatic hydrolysis yield expressed as glucose obtained in the enzymatic hydrolysis divided by the potential glucose in the untreated and pretreated material (%)

Enzymatic Hydrolysis

Figure 7 shows the enzymatic hydrolysis yields determined from the glucose concentration values at each sampling time and the glucose potential content in the untreated and pretreated materials (Table 1). No appreciable reducing glucose accumulation was observed for the untreated material and pretreated solids at temperatures below 140 °C after 12 h even though the enzymatic hydrolysis yield was only approximately 20%. In contrast, after 72 h, the substrates pretreated at the temperatures of 160 °C and 180 °C achieved enzymatic hydrolysis yields in the range of 40 to 60%,

and the sample pretreated at the severest conditions assayed at 200 °C reached the highest yield of 88%. The increase in the enzymatic hydrolysis yields in substrates pretreated between 160 and 200 °C is consistent with the progressive dissolution of hemicelluloses in liquid fraction as pretreatment becomes more severe at those temperatures (Table 1). It should be noted that further increases in pretreatment temperature ranging from 100 °C to 140 °C resulted in a decrease in enzymatic hydrolysis yields. This is an unexpected result, and further experiments are required to explain this phenomenon. This is maybe ascribed to the different cellulose contents of spent solids processed under different operational conditions, and partial cellulose degradation in pretreatments under harsh conditions (Romaní et al. 2010). Nevertheless, the data in Fig. 7 showed excellent digestibility of HCW substrates pretreated above the temperature of 160 °C.

CONCLUSIONS

1. Physicochemical properties and thermal stability of solid residues resulting from HCW pretreatment were analyzed in this study, and it was found that their characteristics were different depending on the temperature of HCW pretreatment.
2. The analysis of the chemical composition indicated that the pretreated solid residues changed a lot from the initial woody biomass. The main effect of HCW pretreatment was the removal of hemicelluloses, which resulted in enriched cellulose and lignin content.
3. From the observation of XRD patterns, it was demonstrated that the cellulosic crystalline structures in the solids could remain with little change in the HCW pretreatment. However, the crystallinity increased from 41.0% in untreated woody powder to 55.5% in the pretreated residues.
4. Solid state NMR analysis showed that wood lignin was broken down by intensive cleavage β-O-4 linkages and Cα-Cβ bonds, and the demethoxylation of lignin led to a more condensed lignin structure.
5. Microscopy studies revealed that HCW pretreatment caused breakage of the matrix fibrous polymers network and partial defibrillation. Moreover, it was evidently observed that the deposition of lignin droplets were produced during pretreatment under hot water conditions, and above 140 °C they can redeposit as spherical droplets on the residual surfaces.
6. Thermal analysis showed that the thermal stability increased in the materials, which was attributed to the removal of hemicelluloses and an increase in crystallinity after pretreatment processing.
7. Enzyme saccharification of HCW pretreated solids at the severest conditions assayed at 200 °C resulted in an enzymatic hydrolysis yield of 88%, which was improved by 3.4-fold in comparison with the untreated material.

ACKNOWLEDGMENTS

The authors are grateful for the financial support of this research from Specific Programs in Graduate Science and Technology Innovation of Beijing Forestry University (BLYJ201110), and partial financial support from Major State Basic Research Projects of China (973-2010CB732204), the National Science Foundation of China (30930073 and 31070526), China Ministry of Education (111), and State Forestry Administration (200804015, 948-2010-4-16).

REFERENCES CITED

Alizadeh, H., Teymouri, F., Gilbert, T. I., and Dale, B. E. (2005). "Pretreatment of switchgrass by ammonia fiber explosion (AFEX)," *Appl. Biochem. Biotechnol.* 121-124, 1133-1141.

Alvira, P., Tomás-Pejó, E., Ballesteros, M., and Negro, M. J. (2010). "Pretreatment technologies for an efficient bioethanol production process basedon enzymatic hydrolysis: A review," *Bioresour. Technol.* 101(13), 4851-4861.

Cara, C., Romero, I., Oliva, J. M., Sáez, F., and Castro, E. (2007). "Liquid hot water pretreatment of olive tree pruning residues," *Appl. Biochem. Biotechnol.* l37-140(1-12), 379-394.

Çetinkol, Ö. P., Dibble, D. C., Cheng, G., Kent, M. S., Knierim, B., Auer, M., Wemmer, D. E., Pelton, J. G., Melnichenko, Y. B., Ralph, J., Simmons, B. A., and Holmes, B. M. (2010). "Understanding the impact of ionic liquid pretreatment on eucalyptus," *Biofuels* 1(1), 33-46.

Chandra, R. P., Bura, R., Mabee, W. E., Berlin, A., Pan, X., and Saddler, J. N. (2007). "Substrate pretreatment: The key to effective enzymatic hydrolysis of lignocellulosics?" *Adv. Biochem. Eng. Biotechnol.* 108, 67-93.

Chen, W. H., Tu, Y. J., and Sheen, H. K. (2010a). "Impact of dilute acid pretreatment on the structure of bagasse for bioethanol production," *Int. J. Energy Res.* 34(3), 265-274.

Chen, X. W., Lawoko, M., and van Heiningen, A. (2010b). "Kinetics and mechanism of autohydrolysis of hardwoods," *Bioresour. Technol.* 101(20), 7812-7819.

Delmotte, L., Ganne-Chedeville, C., Leban, J. M., Pizzi, A., and Pichelin, F. (2008). "CP-MAS ^{13}C NMR and FT-IR investigation of the degradation reactions of polymer constituents in wood welding," *Polym. Degrad. Stab.* 93(2), 406-412.

Donohoe, B. S., Decker, S. R., Tucker, M. P., Himmel, M. E., and Vinzant, T. B. (2008). "Visualizing lignin coalescence and migration through maize cell walls following thermochemical pretreatment," *Biotechnol. Bioeng.* 101(5), 913-925.

Gupta, R., and Lee, Y. Y. (2009). "Pretreatment of hybrid poplar by aqueous ammonia," *Biotechnol. Prog.* 25(2), 357-364.

Inoue, H., Yano, S., Endo, T., Sakaki, T., and Sawayama, S. (2008). "Combining hot-compressed water and ball milling pretreatments to improve the efficiency of the enzymatic hydrolysis of eucalyptus," *Biotechnol. Biofuels* 1(1), article no. 2.

Kobayashi, N., Okada, N., Hirakawa, A., Sato, T., Kobayashi, J., Hatano, S., Itaya, Y., and Mori, S. (2009). "Characteristics of solid residues obtained from hot-compressed-water treatment of woody biomass," *Ind. Eng. Chem. Res.* 48(1), 373-379.

Kristensen, J. B., Thygesen, L. G., Felby, C., Jørgensen, H., and Elder, T. (2008). "Cell-wall structural changes in wheat straw pretreated for bioethanol production," *Biotechnol. Biofuels* 1(1), article no. 5.

Kumar, R., Mago, G., Balan, V., and Wyman, C. E. (2009). "Physical and chemical characterizations of corn stover and poplar solids resulting from leading pretreatment technologies," *Bioresour. Technol.* 100(17), 3948-3962.

Lee, J. M., Jameel, H., and Venditti, R. A. (2010). "A comparison of the autohydrolysis and ammonia fiber explosion (AFEX) pretreatments on the subsequent enzymatic hydrolysis of coastal Bermuda grass," *Bioresour. Technol.* 101(14), 5449-5458.

Lee, S. H., Doherty, T. V., Linhardt, R. J., and Dordick, J. S. (2009). "Ionic liquid-mediated selective extraction of lignin from wood leading to enhanced enzymatic cellulose hydrolysis," *Biotechnol. Bioeng.* 102(5), 1368-1376.

Li, C., Knierim, B., Manisseri, C., Arora, R., Scheller, H. V., Auer, M., Vogel, K. P., Simmons, B. A., and Singh, S. (2010). "Comparison of dilute acid and ionic liquid pretreatment of switchgrass: Biomass recalcitrance, delignification and enzymatic saccharification," *Bioresour. Technol.* 101(13), 4900-4906.

Liu, C. G., and Wyman, C. E. (2004). "The effect of flow rate of very dilute sulfuric acid on xylan, lignin, and total mass removal from corn stover," *Ind. Eng. Chem. Res.* 43(11), 2781-2788.

Liu, S. (2010). "Woody biomass: Niche position as a source of sustainable renewable chemicals and energy and kinetics of hot-water extraction/hydrolysis," *Biotechnol. Adv.* 28(5), 563-582.

Lü, X., and Saka, S. (2010). "Hydrolysis of Japanese beech by batch and semi-flow water under subcritical temperatures and pressures," *Biomass Bioenergy* 34(8), 1089-1097.

Mosier, N. S., Hendrickson, R., Brewer, M., Ho, N., Sedlak, M., Dreshel, R., Welch, G., Dien, B. S., Aden, A., and Ladisch, M. R. (2005). "Industrial scale-up of pH-controlled liquid hot water pretreatment of corn fiber for fuel ethanol production," *Appl. Biochem. Biotechnol.* 125(2), 77-97.

Nuopponen, M. H., Wikberg, H. I., Birch, G. M., Jääskeläinen, A. S., Maunu, S. L., Vuorinen, T., and Stewart, D. (2006). "Characterization of 25 tropical hardwoods with Fourier transform infrared, ultraviolet resonance Raman, and ^{13}C-NMR cross-polarization/magic-angle spinning spectroscopy," *J. Appl. Polym. Sci.* 102(1), 810-819.

Pérez, J. A., González, A., Oliva, J. M., Ballesteros, I., and Manzanares, P. (2007). "Effect of process variables on liquid hot water pretreatment of wheat straw for bioconversion to fuel-ethanol in a batch reactor," *J. Chem. Technol. Biotechnol.* 82(10), 929-938.

Pan, X., Arato, C., Gilkes, N., Gregg, D., Mabee, W., Pye, K., Xiao, Z., Zhang, X., and Saddler, J. (2005). "Biorefining of softwoods using ethanol organosolv pulping: Preliminary evaluation of process streams for manufacture of fuel-grade ethanol and co-products," *Biotechnol. Bioeng.* 90(4), 473-81.

Popescu, C. M., Larsson, P. T., and Vasile, C. (2011). "Carbon-13 CP/MAS solid state NMR and X-ray diffraction spectroscopy studies on lime wood decayed by *Chaetomium globosum*," *Carbohydr. Polym.* 83(2), 808-812.

Romaní, A., Garrote, G., Alonso, J.L., and Parajó, J.C. (2010). "Bioethanol production from hydrothermally pretreated *Eucalyptus globulus* wood," *Bioresour. Technol.* 101(22), 8706-8712.

Sassner, P., and Zacchi, G., (2008). "Integration options for high energy efficiency and improved economics in a wood-to-ethanol process," *Biotechnol. Biofuels* 1(1), article no. 4.

Segal, L., Creely, L., Martin, A. E., and Conrad, C. M. (1959). "An empirical method for estimating the degree of crystallinity of native cellulose using X-ray diffractometer," *Text. Res. J.* 29(10), 786-794.

Selig, M. J., Viamajala, S., Decker, S. R., Tucker, M. P., Himmel, M. E., and Vinzant, T. B. (2007). "Deposition of lignin droplets produced during dilute acid pretreatment of maize stems retards enzymatic hydrolysis of cellulose," *Biotechnol. Prog.* 23(6), 1333-1339.

Selig, M., Weiss, N., and Ji, Y. (2008). "Enzymatic saccharification of lignocellulosic biomass," In: Laboratory Analytical Procedure (LAP), NERL/TP-510-42629, National Renewable Energy Laboratory Golden, CO.

Singh, S., Simmons, B. A., and Vogel, K. P. (2009). "Visualization of biomass solubilization and cellulose regeneration during ionic liquid pretreatment of Switchgrass," *Biotechnol. Bioeng.* 104(1), 68-75.

Sluiter, A., Hames, B., Ruiz, R., Scarlata, C., Sluiter, J., and Templeton, D. (2006). "Determination of sugars, bioproducts, and degradation productsd in liquid fraction process samples," In: Laboratory Analytical Procedure (LAP), NREL/TP-510-42623, National Renewable Energy Laboratory Golden, CO.

Sluiter, A., Hames, B., Ruiz, R., Scarlata, C., Sluiter, J., Templeton, D., and Crocker, D. (2008). "Determination of structural carbohydrates and lignin in biomass," In: Laboratory Analytical Procedure (LAP), NREL/TP-510-42618, National Renewable Energy Laboratory Golden, CO.

Spinacé, M. A. S., Lambert, C. S., Fermoselli, K. K. G., and De Paoli, M. A. (2009). "Characterization of lignocellulosic curaua fibres," *Carbohydr. Polym.* 77(1), 47-53.

Vlasenko, E. Y., Ding, H., Labavitch, J. M., and Shoemaker, S. P. (1997). "Enzymatic hydrolysis of pretreated rice straw," *Bioresour. Technol.* 59(2-3), 109-119.

Wang, B., Wang, X. J., and Feng, H. (2010). "Deconstructing recalcitrant *Miscanthus* with alkaline peroxide and electrolyzed water," *Bioresour. Technol.* 101(2), 752-760.

Wikberg, H., and Maunu, S. L. (2004). "Characterisation of thermally modified hard- and softwoods by ^{13}C CPMAS NMR," *Carbohydr. Polym.* 58(4), 461-466.

Wyman, C. E., Dale, B. E., Elander, R. T., Holtzapple, M., Ladisch, M. R., and Lee, Y. Y. (2005). "Coordinated development of leading biomass pretreatment technologies," *Bioresour. Technol.* 96(18), 1959-1966.

Xu, Y. J., Li, K. C., and Zhang, M. Y. (2007). "Lignin precipitation on the pulp fibers in the ethanol-based organosolv pulping," *Colloids Surf. A: Physicochem. Eng. Aspects* 301(1-3), 255-263.

Yang, H. P., Yan, R., Chen, H. P., Zheng, C. G., Lee, D. H., and Liang, D. T. (2006). "In-depth investigation of biomass pyrolysis based on three major components: Hemicellulose, cellulose and lignin," *Energ. Fuel.* 20(1), 388-393.

Yu, G., Yano, S., Inoue, H., Inoue, S., Endo, T., and Sawayama, S. (2010). "Pretreatment of rice straw by a hot-compressed water process for enzymatic hydrolysis," *Appl. Biochem. Biotechnol*. 160(2), 539-551.

Yu, Y., and Wu, H.W. (2010). "Understanding the primary liquid products of cellulose hydrolysis in hot-compressed water at various reaction temperatures," *Energy. Fuel.* 24(3), 1963-1971.

Yu, Y., and Wu, H.W. (2011). "Effect of ball milling on the hydrolysis of microcrystalline cellulose in hot-compressed water," *AIChE Journal.* 57(3), 793-800.

Yu, Y., Lou, X., and Wu, H. W. (2008). "Some recent advances in hydrolysis of biomass in hot-compressed water and its comparisons with other hydrolysis methods," *Energ. Fuel.* 22(1), 46-60.

Zeng, M. J., Mosier, N. S., Huang, C. P., Sherman, D. M., and Ladisch, M. R. (2007). "Microscopic examination of changes of plant cell structure in corn stover due to hot water pretreatment and enzymatic hydrolysis," *Biotechnol. Bioeng.* 97(2), 265-278.

Zhu, W., Zhu, J. Y., Gleisner, R., and Pan, X. J. (2010). "On energy consumption for size-reduction and yields from subsequent enzymatic saccharification of pretreated lodgepole pine," *Bioresour. Technol.* 101(8), 2782-2792.

Zhu, Z. G., Sathitsuksanoh, N., Vinzant, T., Schell, D. J., McMillan, J. D., and Zhang, Y. -H. P. (2009). "Comparative study of corn stover pretreated by dilute acid and cellulose solvent-based lignocellulose fractionation: Enzymatic hydrolysis, supramolecular structure, and substrate accessibility," *Biotechnol. Bioeng.* 103(4), 715-724.

Article submitted: December 28, 2010; Peer review completed: February 25, 2011; Revised version received and accepted: March 17, 2011; Published: March 20, 2011; with minor corrections republished March 31, 2011.